Hot Hypernucleus Formation in High-Energy Photonuclear Reactions

M. Gonçalves[1], E.C. de Oliveira[2], E.L. Medeiros[2], S. de Pina[3], and S.B. Duarte[2]

[1]*Instituto de Radioproteção e Dosimetria, Av. Salvador Allende, Rio de Janeiro, Brazil, 22780-160*

[2]*Centro Brasileiro de Pesquisas Físicas, Rua Dr. Xavier Sigaud 150, Urca, Rio de Janeiro, Brazil, 22290-180*

[3]*Instituto Militar de Engenharia, Pça. Gen. Tibúrcio 80, Praia Vermelha, Rio de Janeiro, Brazil, 22290-270*

Received on 10 October, 2003.

The probability of a compound residual hot hypernucleus formation at the end of pre-equilibrium phase of high energy photonuclear reactions is calculated with a time dependent Monte Carlo Multicollisional Cascade (MCMC) approach. The emission of hadrons during the rapid phase of the reaction is discussed and characteristics of the residual nucleus are obtained. Results for mass and charge distributions of the formed hot hypernucleus are shown and its excitation energy is discussed.

A renewed interest in the subject of strangeness production in proton-nucleus, pion-nucleus, and kaon-nucleus reactions appeared since the observation of hypernucleus bound states for some nuclei such as ${}^{10}_{\Lambda}$B, ${}^{12}_{\Lambda}$C, ${}^{28}_{\Lambda}$Si, ${}^{89}_{\Lambda}$Y, ${}^{139}_{\Lambda}$La, ${}^{208}_{\Lambda}$Pb, ${}^{209}_{\Lambda}$Bi, and ${}^{238}_{\Lambda}$U [1-7]. The energy level density, branching ratio of non-mesonic to mesonic decays, and hypernucleus lifetime have been investigated. Another important subject is the effect of the Pauli exclusion principle on the suppression of mesonic decay in favor of the non-mesonic decay of hyperons, mainly for heavy target nuclei. Moreover, the many-body re-scattering Λ-N also contributes to the thermalization of the hyperon, and increases its probability of being confined in the nuclear environment [6, 7]. Indeed, static calculations based on studies of the hyperon-nucleon potential[8, 9], chiral perturbation theory [10], and statistical models[11] have provided some insight on the properties of hypernuclei such as their mass shifts, wave functions, fissioning path, and attachment probabilities of hyperons in nuclei.

Theoretical and experimental interest in photonuclear kaon-production reactions has grown from the observation of new nuclear Λ-bound states, which have been experimentally detected through the excitation of the target nucleus by incident photons with energy in the range 0.8–1.4 GeV [4, 12]. Also, new phenomena related to the inclusion of a Λ in the nuclear structure, such as the halo effects [13], have been observed. A typical example is ${}^{6}_{\Lambda}$He which is bound by 0.17 MeV against the breaking into ${}^{5}_{\Lambda}$He + n[13]**,** being ${}^{5}_{\Lambda}$He unbound by 0.89 MeV above the threshold for ${}^{5}_{\Lambda}$He $\rightarrow \alpha + n$ reaction. Another example is the ${}^{13}_{\Lambda}$C, which can be thought of as a Λ-particle attached to the ^{12}C nucleus, and the Λ-bound p-states are 11 MeV above the s-state. By measuring the spin-orbit splitting, and the gamma emission during the transition $p \rightarrow s$, one can obtain information on the signature of the hypernucleus existence [14].

In the photomesonic energy region, the gamma-nucleus reaction has been explored in the framework of a two-step interaction model. First, a rapid intranuclear cascade is developed through a sequence of hadronic binary collisions. Subsequently, the hot residual nucleus slowly reaches its final configuration through a sequence of particle-evaporation processes in competition with the residual-nucleus fission process.

We have shown that quasi-free kaon production in photonuclear reactions can be an important issue to determine the strangeness content of the residual nuclei at the end of the rapid cascade phase[15]. These reactions permit to study the *in-medium* effects on the photonuclear absorption and the strangeness-production mechanism. The many-body cascade calculation proposed in Refs.[15, 16] for the rapid phase of the photonuclear reaction takes into account the dynamical evolution of the multicollisional processes. The dynamical characteristics of the MCMC calculation allow for a time-dependent analysis of the rapid and pre-equilibrium phases within a single theoretical approach, in contrast with standard calculations [12, 17, 18]. The final residual-nucleus configuration at the end of the rapid phase is the starting point for the subsequent evaporation phase of the photonuclear reaction. The excitation energy of the residual hypernucleus is determined taking into account the energy distribution of bound baryons at the end of the pre-equilibrium phase. The distribution is fitted to a finite temperature Fermi distribution, from which the diffusion parameter is extracted as the nuclear thermal excitation. Excitation energy can be obtained considering events with pion and kaon production, as well as for events with only kaon production. This subject is discussed in our previous work (see Fig.4 of Ref. [15]).

Pion and kaon production occurs only during the rapid phase of the photonuclear reaction. They are accompanied by energetic baryons escaping from the formed excited nuclear system. With MCMC approach we are also able to discuss pion and kaon multiplicity, their spectra near and above the threshold, as shown in [16, 19, 20] and references therein. The existing amount of data for pion production al-

lowed us to fix some parameters of the MCMC calculation, giving us confidence on the results offered by the developed approach and code. With the purpose to study kaon production, strange particle processes were introduced in the MCMC. The result of this extended model was confronted with the available experimental data for carbon, presenting a satisfactory agreement (Fig 3. of Ref. [15]). Since the MCMC model is designed for intermediate and heavy nuclei, the above result stimulated us to extract results for hypernucleus formation using carbon and heavier targets. We determined the hot residual hypernuclei configuration at the end of the rapid and pre-equilibrium phase of the reaction. These results can not be directly compared with experimental data. However, this is an important and necessary step to be used as input to the nuclear evaporation phase, giving final predictions to experimental data.

The nuclear reaction starts with the primary photonuclear interaction producing pions or kaons in the following channels:

$$\gamma\, N \;\rightarrow\; N\,\pi\,, \tag{1}$$
$$\gamma\, N \;\rightarrow\; \pi\,\Delta \rightarrow \pi\,\pi\,N\,, \tag{2}$$
$$\gamma\, N \;\rightarrow\; K^{+}\,\mathrm{Y}\,. \tag{3}$$

Direct one-pion production is introduced through Eq. (1). The production of two pions is mediated by a delta resonance, Eq. (2). Cross sections for these two photomesonic processes have been taken from Ref. [21]. The kaon produced through Eq. (3) is accompanied by a hyperon, Y (Λ or Σ); the cross section for the γ-p channel has been taken from Ref. [22]. Due to the lack of experimental information, the cross section for the γ-n reaction producing K^+ has been considered equal to that one for the γ-p interaction with the same total isospin in the final state, γp$\rightarrow K^{+}\Sigma^{0}$. In the energy range of interest, the energy dependence of the experimental cross sections of the γ-p interactions is parametrized by fifth-degree polynomials (see Ref.[15]).

Following the primary γ-nucleon interaction, the calculation scheme tracks the sequence of binary collisions among the particles of the overall system [19,20]. Hypernucleus production and its thermalization are studied by including the following elastic and inelastic elementary processes in the multicollisional intranuclear cascade model:

$$B_1\,B_2 \;\rightarrow\; B_1\,B_2\,, \tag{4}$$
$$N\,N \;\rightarrow\; N\,\Delta\,, \tag{5}$$
$$N\,\Delta \;\rightarrow\; N\,N\,, \tag{6}$$
$$\Delta \;\rightarrow\; \pi\,N\,, \tag{7}$$
$$\pi\,N \;\rightarrow\; \Delta\,, \tag{8}$$
$$\Lambda\,N \;\rightarrow\; \Lambda\,N\,, \tag{9}$$

where B_1 and B_2 stand for baryons in general, and N stands for nucleons. The cross sections for the baryon-baryon elastic processes [Eq. (4)] are taken from reference [23]. For the delta-formation process [Eq. (5)], the VerWest parametrization of the cross sections [24] has been used, while the extended detailed-balance relation of Refs. [20, 25] has been used for the inverse process [Eq. (6)]. The lifetime associated with the delta-resonance decay, Eq. (7), is governed by the characteristic exponential law. Finally, the cross section of the pion absorption process [Eq. (8)] has been taken from a Breit-Wigner distribution function, scaled by the maximum experimental value for the inelastic cross section of the pion-nucleon reaction [26]. We have also considered the elastic process hyperon-nucleon, Eq. (9), whose cross section has been taken from reference [27]. The inclusion of these two processes is indeed relevant to the thermalization of the hyperon energy, as will be discussed later.

The baryons in the target nucleus are confined within a potential well with a characteristic depth of $V_N = 43$ MeV for nucleons, and $V_Y = V_N/3$ for hyperons. The binding-energy effect on the baryon kinematics is included by considering effective masses, μ_N and μ_Y, in the dispersion relation for bound baryons

$$E_i^2 = p_i^2 + \mu_i^2\,. \tag{10}$$

During the time evolution of the cascading system, the processes of reflection and refraction of bound baryons — including the hyperon produced in the primary interaction— on the nuclear potential surface [19, 28] are taken into account. The hyperon produced in the primary interaction escapes from the nucleus whenever its kinetic energy is higher than the Coulomb barrier or when the hyperon tunnels this barrier. Otherwise, the hyperon is kept bound until the end of the rapid and pre-equilibrium phases of the photonuclear reaction.

The Pauli exclusion principle is included in the present calculation by using the same prescription of our earlier works [15,16], where collisions with relative kinetic energy smaller than the Fermi energy (*soft collisions*) are forbidden. We emphasize that this prescription has been used for both the baryons in the final state of baryon-baryon interactions and the nucleon in the final state of the delta-resonance decay. The nucleon scattered in the primary interaction is also required to satisfy the Pauli exclusion principle.

It is important to remark that the medium effect on baryon propagation is represented by the simultaneous action of the following ingredients introduced into the Monte Carlo simulation: a) the Pauli blocking to baryon-baryon individual collisions described above; b) changes in the kinematic relation of baryon-baryon collisions, due to the use of an effective mass parameter (introduced to take into account mean field correction for binding baryons mass); c) transients change at nuclear surface represented by the confining potential well together with the coulomb barrier for charged baryons at geometric boundaries of the nucleus. During its propagation along the nuclear medium the hyperon suffers successive binary collisions, which are less blocked (we have only one nucleon in the final state) in comparison with a successive nucleon-nucleon collision (with two nucleons being blocked) along a nucleon propagation with same energy. Mean free path is smaller for hyperons than for nucleons propagating in the nucleus. Consequently, the hyperon excitation energy is redistributed to the medium particles easier than in the case of excited nucleons, increasing the chances of low energy hyperon formed in the primary interaction to be kept in the hot residual nuclear system formed.

The main purpose of the present work is to discuss the hypernucleus formation in γ-nucleus reactions at incident energies in the range 0.8–1.4 GeV. We first concentrate attention on estimating the chances for hypernucleus formation in these reactions. In order to have this estimate we define the inclusive probability of hyperons to be incorporated to the residual nucleus at the end of the rapid reaction phase as

$$\mathcal{P}_{\mathcal{Y}} = \frac{\sum \mathcal{N}_{\mathcal{Y}}(\mathcal{Z},\mathcal{A})}{\mathcal{N}_{\mathcal{R}}}, \qquad (11)$$

where N_Y is the number of residual hypernuclei with charge Z and baryonic number A occurred after N_R events generated in the Monte Carlo simulation of the photonuclear reaction. In Fig. 1-a, $\mathcal{P}_{\mathcal{Y}}$ is displayed as a function of the incident energy for γ-carbon (solid line), γ-neon (dashed line), γ-calcium (dotted line), and γ-nickel (dot-dashed line) reactions. As it is clear from Fig.1-a, this quantity increases with incident energy, being steeper for heavier nuclei.

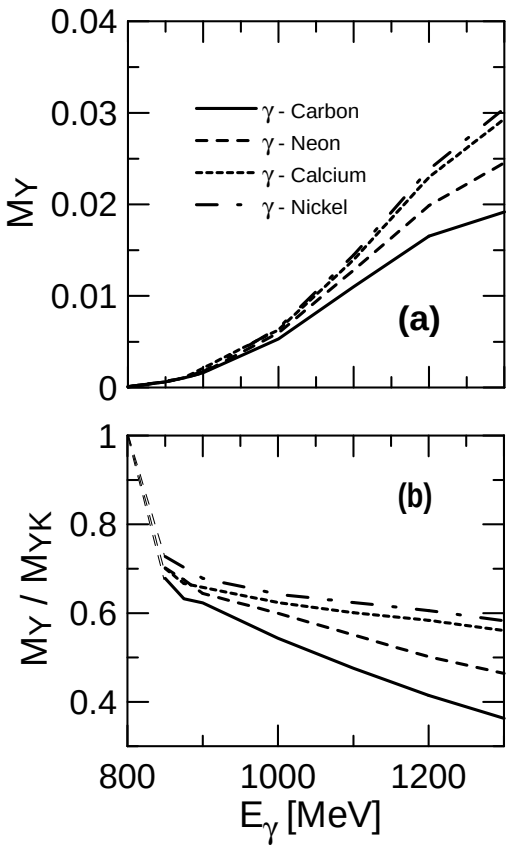

Figure 1. Hypernucleus multiplicity (a), and M_Y/M_{K^+} ratio (b), as a function of incident energy for ^{12}C(γ,K^+) (solid lines), ^{20}Ne(γ,K^+) (dashed lines), ^{40}Ca(γ,K^+) (dotted lines), and ^{58}Ni(γ,K^+) (dot-dashed lines) reactions. In (b) the short dashed lines linking the curves to the vertical axis do not result from calculation (see text for more details).

Another important quantity to be explored is the ratio of the number of events with bound hyperons, M_Y, to the number of events in which hyperons are produced but not necessarily are bound in the residual nucleus, M_{YK}. The ratio M_Y/M_{YK}, shown in Fig. 1-b, decreases with the photon energy. As already asserted when discussing Fig. 1-a, by increasing the incident energy the number of bound hyperons does not follow the number of produced hyperons, *i.e.*, although more hyperons are formed, many of them are not kept bound in the residual nucleus. Regarding the target-nucleus mass, the ratio M_Y/M_{YK} is, in general, larger for heavy nuclei than for light ones. The baryon-baryon multicollisional processes reduce the hyperon kinetic energy (decreasing the probability of its direct ejection from the nuclear medium), so the increase of the number of nucleons in the target increases the probability of the hyperon to be bound in the residual nucleus. At energies close to the hyperon photomesonic threshold (E_γ lower than 850 MeV), it is very hard to obtain statistical convergence by Monte Carlo calculation for the ratio M_Y/M_{YK}. However, hyperons formed at threshold are almost at rest and the probability of being bound is near to one. In Fig. 1-b we connected the extremes of the calculated curves to the value one on the vertical axis by straight lines, to give the trends.

We previously showed that the hyperon production in the primary interaction suppresses the ejection of nucleons by the target nucleus [16]. A stronger suppression is expected to occur when the hypernucleus production takes place. Therefore, it is important to investigate the residual-nucleus mass and charge distributions at the end of the rapid phase of the reaction. These distributions are relevant to the evaporation phase of the photonuclear reaction, and the number of baryons in the nuclear matter is determinant in deciding the clustering-fissioning path chosen by the system. Also, due to the low kinetic content of the bound hyperon, we expect that this hyperon, once kept bound in the rapid phase of the reaction, will not be able to escape from the nuclear mean field during the evaporation phase.

Finally, in Fig.2 we show the residual nucleus distributions in the (Z,A)-plane for γ-Carbon (first row), γ-Aluminum (second row), and γ-Nickel (last row) at 1.2 GeV incident photon energy. In the first column it is shown the distribution for inclusive meson production events (either a pion or a kaon is produced in the primary interaction). In the middle column we show distributions taking into account only events with hyperon production in the primary interaction, however without considering if the hyperon is kept bound or not. In the last column, it is shown the distribution for events in which the hyperon is maintained in the nuclear medium until the end of the pre-equilibrium phase, e.g., events with a hot hypernucleus formed. Considering distributions in each row (although presenting different spreading) they have roughly the same centroid (whose location depends on the photon incident energy). Concerning the height of distribution peaks in the last two columns, we note that for γ-Carbon and γ-Nickel reactions approximately 1/2 of formed hyperon in the primary photon interaction left the nucleus during the pre-equilibrium phase. This fraction is an intricate function of target mass and photon incident energy, being reduced to 1/3 when comparing the two columns for γ-Aluminum reaction (second row in Fig. 2).

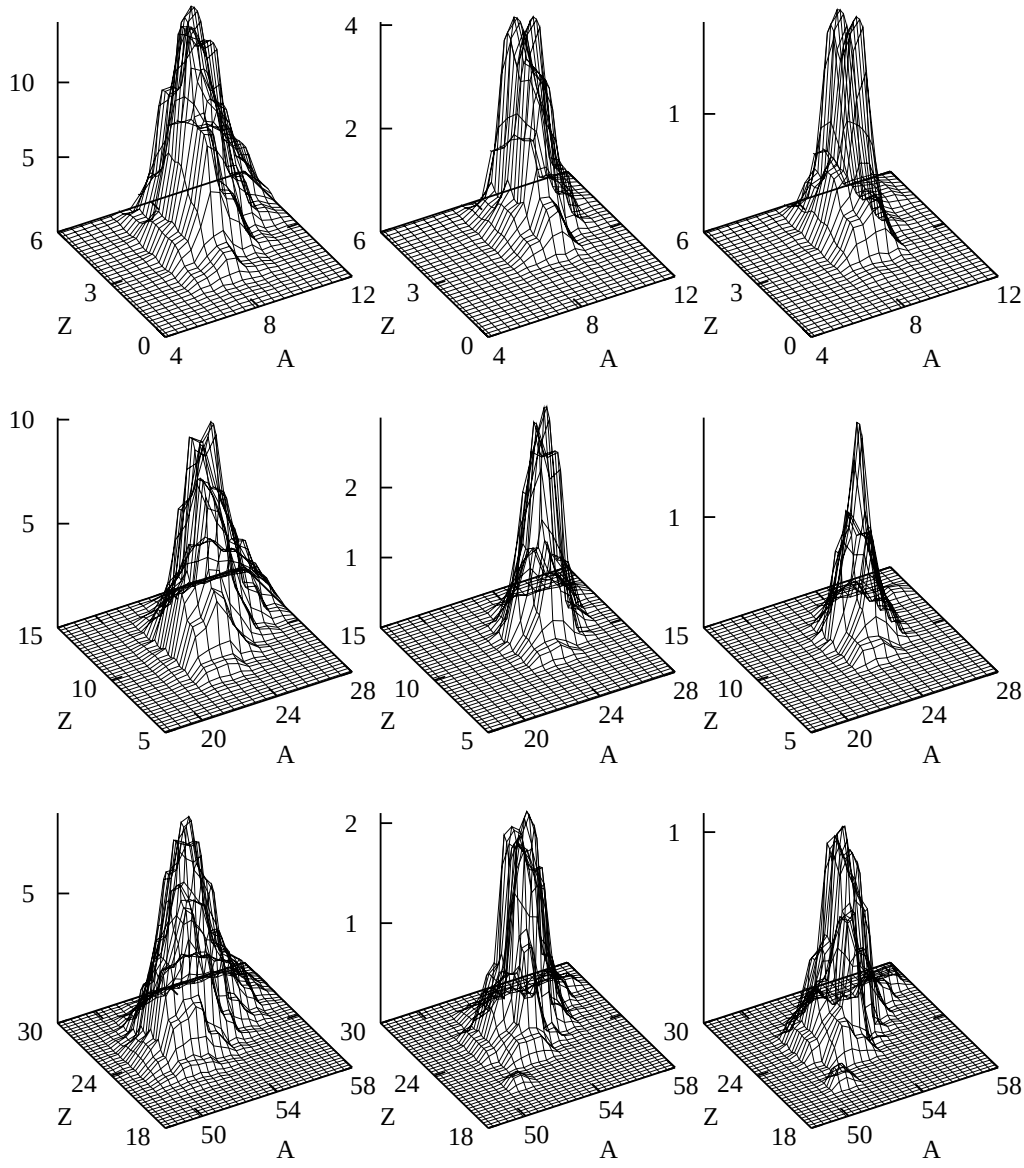

Figure 2. Residual nucleus mass and charge distributions for γ-Carbon (first row), γ-Aluminum (second row), and γ-Nickel (last row) at 1.2 GeV incident photon energy. In the first column we display results for events inclusive in meson production (either a pion or a kaon is produced in the primary interaction). In the middle column we show distributions of mass and charge considering only events with hyperon production in the primary interaction, however disregarding if the hyperon is kept bound or not. In the last column the distribution for events having a bound hyperon formed at the end of pre-equilibrium phase of the residual hot nucleus. The results in columns are multiplied, respectively, by 10^2, 2 x10^4, and 2 x 10^4.

References

[1] K. Kubota *et al*., Nucl. Phys. A**602**, 327 (1996).

[2] T. Hasegawa *et al.*, Phys. Rev. C**53**, 1210 (1996).

[3] O. Hashimoto, Hyper. Inter. **103**, 245 (1996).

[4] H. Yamazaki *et al*., Phys. Rev. C**52**, R1157 (1995).

[5] H. Ohm *et al.*, Phys. Rev. C**55**, 3062 (1997) .

[6] H. Noumi *et al.*, Phys. Rev. C**52**, 2936 (1995).

[7] S. Ajimura *et al.*, Nucl. Phys. A**577**, 271c (1994).

[8] H. Outa, Hyper. Inter. **103**, 227 (1996).

[9] I. Kamagai-Fuse, S. Okabe, and Y. Akaishi, Phys. Rev. C**54**, 2843 (1996).

[10] M. Savage and M.B. Wise, Phys. Rev. D**53**, 349 (1996).

[11] F.F. Karpeshin, C.G. Koutroulos, and M.E. Grypeos, Nucl. Phys. A**595**, 209 (1995).

[12] K. Maeda *et al*., Nucl. Phys. A**577**, 277c (1994).

[13] K. Riisager, Rev. Mod. Phys. **66**, 1105 (1994).

[14] M. May *et al.*, Phys. Rev. Lett. **78**, 4343 (1997).

[15] S. de Pina, E.C. de Oliveira, E.L. Medeiros, S.B. Duarte, and M. Gonçalves, Phys. Lett. B**434**, 1 (1998).

[16] M. Gonçalves, S. de Pina, D.A. Lima, W. Milomen, E.L. Medeiros, and S.B. Duarte, Phys. Lett. B**406**, 1 (1997).

[17] V.S. Barashenkov, F.G. Gereghi, A.S. Iljinov, G.G. Jonsson, and V.D. Toneev, Nucl. Phys. A**231**, 462 (1974).

[18] H.W. Bertini, Phys. Rev. **131**, 1801 (1963).

[19] E.L. Medeiros, S.B. Duarte, and T. Kodama, Phys. Lett. B**203**, 205 (1988).

[20] M. Gonçalves, E.L. Medeiros, and S.B. Duarte, Phys. Rev. C**55**, 2625 (1997).

[21] H.G. Hilpert *et al*., Phys. Lett. B**27**, 474 (1968).

[22] M. Bockhost *et al*., Z. Phys. C**63**, 37 (1994).

[23] O. Benary, L.R. Price, and G. Alexander, "NN and ND interactions (above 0.5 GeV/c)", University of California, Berkeley, Report No. UCRL-20000 NN, 1970.

[24] B.J. VerWest and R.A. Arndt, Phys. Rev. C**25**, 1979 (1982).

[25] Gy. Wolf, W. Cassing, and U. Mosel, Nucl. Phys. A**545**, 139c (1992).

[26] Gy. Wolf, G. Batko, W. Cassing, U. Mosel, K. Niita, and M. Schäfer, Nucl. Phys. A**517**, 615 (1990).

[27] K. Hollinde, Nucl. Phys. A**547**, 255c (1992).

[28] Y. Kitazoe, M. Sano, Y. Yamamura, H. Furutani, and K. Yamamoto, Phys. Rev. C**29**, 828 (1984).